

# Reconstructing a Heavy Neutral Lepton at the LHC

Pablo de la Torre, Manuel Masip, Fuensanta Vilches

*Departamento de Física Teórica y del Cosmos  
Universidad de Granada, E-18071 Granada, Spain*

`pdelatorre@ugr.es`   `masip@ugr.es`   `fuenvilches@ugr.es`

## Abstract

Heavy lepton singlets  $N$  slightly mixed with a standard neutrino  $\nu_\ell$  are usually searched for at the LHC in the trilepton plus  $p_T^{\text{miss}}$  channel:  $pp \rightarrow W^+ \rightarrow \ell^+ N$  with  $N \rightarrow \ell^- W^+ \rightarrow \ell^- \ell'^+ \nu$ . We show that, although the longitudinal momentum of the final  $\nu$  escapes detection, the mass of the heavy lepton can be reconstructed. This possibility has been overlooked in recent LHC searches. We show that for  $m_N \approx 90\text{--}130$  GeV and the current luminosity (138  $\text{fb}^{-1}$  at 13 TeV), the bounds at the LHC could be competitive with the  $|V_{\ell N}|^2 \lesssim 10^{-3}$  limits from flavor and electroweak precision data.

# 1 Introduction

Heavy neutral leptons (HNL) provide the simplest UV completion of the Standard Model (SM) that is able to generate the dim-5 Weinberg operator [1], which arguably makes them the most motivated scenario for BSM physics [2–8]. Let us briefly discuss a minimal setup (see also the majoron model in [9] or the dark matter model in [10]) using 2-component spinors\*.

To explain neutrino masses we need at least two bi-spinors  $(N, N^c)$  of opposite lepton number  $L = \pm 1$  combined into a Dirac field of mass  $M$ . Assuming no extra Higgses, lepton-number conservation and only  $\text{dim} \leq 4$  operators we have

$$-\mathcal{L} \supset M N N^c + y_\nu H L N^c + \text{h.c.}, \quad (1)$$

where  $H = (h^+ \ h^0)$ ,  $L = (\nu \ \ell)$  and we have redefined the 3 lepton doublets to obtain the flavor combination in the Yukawa. After electroweak (EW) symmetry breaking the neutrino mass matrix reads

$$\mathcal{M} = \begin{pmatrix} & & \cdot & 0 \\ 0 & & \cdot & 0 \\ & & \cdot & m \\ \cdot & \cdot & \cdot & M \\ 0 & 0 & m & M & \cdot \end{pmatrix}, \quad (2)$$

where  $m = y_\nu v / \sqrt{2}$  and the dots indicate terms forbidden by  $L$ . This rank-2 matrix implies a Dirac field  $(N', N^c)$ , with  $N' = c_\alpha N + s_\alpha \nu_3$ , of mass  $m_N = \sqrt{M^2 + m^2}$  plus three massless neutrinos. The neutrino  $\nu'_3 = -s_\alpha N + c_\alpha \nu_3$  is massless but has now a small component  $s_\alpha = m / \sqrt{M^2 + m^2}$  along the sterile flavor  $N$ .

In order to get non-zero masses we need to break  $L$ : we can add small Majorana masses ( $\mu_{1,2} \ll M$ ,  $\Delta L = 2$ ) for the two heavy modes and suppressed Yukawas ( $\tilde{y}_\nu \ll y_\nu$ ,  $\Delta L = 1$ ) for  $N$ , implying

$$\mathcal{M} = \begin{pmatrix} & 0 & 0 \\ 0 & \mu_3 & 0 \\ & \mu'_3 & m \\ 0 & \mu_3 & \mu'_3 & \mu_1 & M \\ 0 & 0 & m & M & \mu_2 \end{pmatrix}. \quad (3)$$

---

\*In this notation  $\chi$  is a left-handed spinor and its conjugate contravariant  $\bar{\chi}$  is right handed (we omit Lorentz indexes). For example, to define the electron we need two left handed spinors ( $e$  and  $e^c$ ) of opposite charge; a mass term reads  $m(ee^c + \bar{e}\bar{e}^c) = m\bar{\Psi}_e\Psi_e$ , where  $\Psi_e$  is the 4-component electron in the chiral representation of  $\gamma^\mu$ :  $\Psi_e = \begin{pmatrix} e \\ \bar{e}^c \end{pmatrix}$  and  $\bar{\Psi}_e = (e^c \ \bar{e})$ .

The mass  $\mu_1$  increases in one unit the rank of  $\mathcal{M}$  and defines an inverse seesaw with  $m_{\nu_3} \approx \mu_1(m/M)^2$  [11]. The term  $\mu_2$  does not give mass to a second standard neutrino, it just breaks the degeneracy between the two (now Majorana) heavy neutrinos. The term  $\mu_3 = \tilde{y}_\nu v/\sqrt{2}$  is then necessary to give a mass  $m_{\nu_2} \approx \mu_3^2/\mu_1$  to  $\nu'_2$ , with  $\nu'_1$  staying massless. Alternatively,  $\mu_3$  could be forbidden by a discrete symmetry and  $m_{\nu_2}$  obtained by adding a second heavy neutrino pair (*i.e.*, an inverse seesaw for the two massive neutrino families).

The mass parameters  $M$  and  $\mu_{1,2}$  above are not EW, and the matrix in Eq. (3) may accommodate any values between  $10^{-3}$  and  $10^{15}$  GeV: any HNL mass seems equally *natural*, and only the data may have a say about nature's choice. Masses larger than the TeV, however, imply a very small mixing  $s_\alpha$  and thus a decoupled HNL. In particular, the usual seesaw mechanism is obtained if the three mass parameters and the Yukawa couplings are all unsuppressed, *e.g.*,  $M, \mu_{1,2} \approx 10^{10}$  GeV and  $m, \mu_3 \approx 1$  GeV.

The possibility of two Majorana HNLs at the TeV scale with sizeable heavy-light mixings (*e.g.*,  $m = 10$  GeV,  $\mu_{1,2} \approx 1$  TeV and  $M = 0$ ) requires a fine tuning ( $m^2/\mu_2 + \mu_3'^2/\mu_1 \approx 10^{-8}m^2/\mu_2$ ) that is not stable under radiative corrections. If one of the HNLs is significantly heavier than the other one, the cancelation forces its mixing to be smaller and the model reduces to a single Majorana HNL mixed with a combination of the standard neutrinos. Therefore, although throughout our analysis we will assume a quasi-Dirac HNL  $N$ , we will also discuss this fine tuned Majorana case.

The heavy-light mixing  $s_\alpha$  defines then the couplings of  $\nu_\ell$  and  $N$  to the  $W^\pm$  and  $Z$  bosons (we drop the prime to denote mass eigenstates). In particular,  $\nu_\ell$  will see its gauge couplings reduced by a factor of  $c_\alpha$  whereas  $N$  will now couple to the  $W$  with a strength proportional to  $V_{\ell N} \approx s_\alpha$ . The model also implies heavy-light couplings both to the  $Z$  boson ( $\propto s_\alpha c_\alpha$ ) and to the Higgs boson ( $y_\nu = \sqrt{2}s_\alpha M/v$ ).

Collider bounds on  $|V_{\ell N}|^2$  may be obtained at energies below or above  $m_N$ . At lower energies the HNL is not produced and the bounds are based on observables like the universality of weak interactions, precision observables related to  $\mu$  decays (the mixing with  $\nu_\mu$  changes the definition of  $G_\mu$ ), the invisible width of the  $Z$  boson or one-loop flavor changing processes like  $\mu \rightarrow e\gamma$ . A global fit of these observables sets limits on  $|V_{\ell N}|^2$  ranging from  $10^{-2}$  to  $10^{-4}$ , being the most stringent ones for  $\ell = \mu$  [12–14].

Here we will discuss higher energy processes with the direct production of the HNL. The current collider limits for  $m_N > M_W$  have been obtained by CMS in the trilepton channel at the LHC [15, 16] and by L3 at LEP [17] (see the dominant diagrams in Fig. 1), in this second case only for  $\ell = e$ . We will focus on the trilepton channel. We will show that, although the longitudinal momentum of the  $\nu$  escapes detection, the mass  $m_N$  of the HNL can be

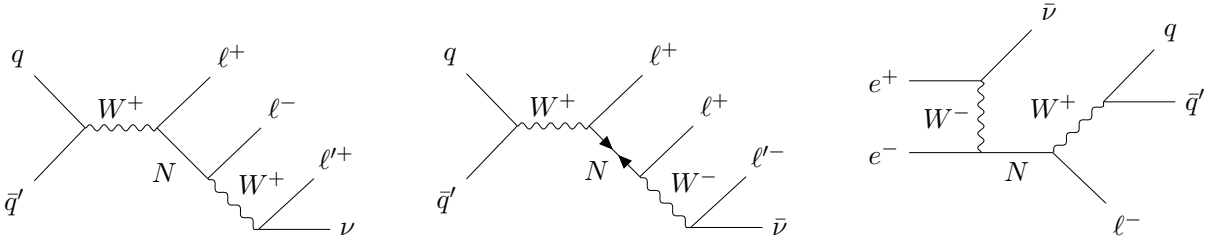


Figure 1: Dominant diagrams in  $N$  searches at CMS (Dirac or Majorana) and L3.

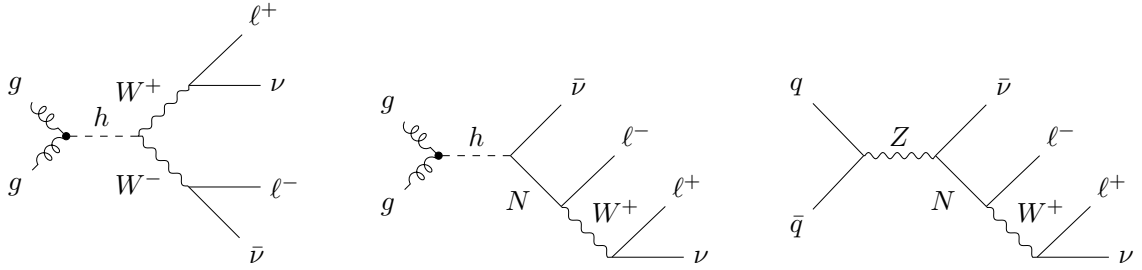


Figure 2: Higgs to  $W^+W^-$  in the SM and possible HNL contributions to dilepton plus  $p_T^{\text{miss}}$ .

reconstructed. We will also comment on the possible effects introduced by a HNL in Higgs searches at the LHC. In particular, notice (see Fig. 2) that the dilepton plus missing  $p_T$  signal from  $h \rightarrow WW^*$  observed at CMS coincides with the one from  $h, Z \rightarrow \nu N$ , although the kinematics in each process is obviously different.

## 2 HNL at the LHC

To study the signal of a HNL at the LHC we first produce an UFO file [18] with FeynRules [19] that includes the new interactions, then we generate signal and background events with MadGraph5 [20] + Pythia [21], and finally we analyze the results with routines based on FasJet [22], ROOT [23] and HepMC [25].

Let us consider a 90, 110 or 130 GeV HNL with, in all cases, a mixing  $|V_{\mu N}|^2 = 10^{-3}$  with the muon flavor<sup>†</sup>. For  $138 \text{ fb}^{-1}$  at 13 TeV, our simulation estimates, respectively, 1021, 317 or 153 HNL events giving two opposite sign muons, an electron and  $\vec{p}_T^{\text{miss}}$ .

$$pp \rightarrow \mu^\pm N \rightarrow \mu^\pm \mu^\mp W^\pm \rightarrow \mu^\pm \mu^\mp e^\pm \nu. \quad (4)$$

In the simulation we have included the events where the final electron comes from the

<sup>†</sup>As we will see, for this mixing and the current luminosity the LHC can not access larger masses.

leptonic decay of a tau lepton (*i.e.*, the  $\ell'^+$  in Fig. 1 may be an  $e^+$  or a  $\tau^+$  decaying into  $\bar{\nu}_\tau e^+ \nu_e$ ). We then apply the cuts defined in [16], namely, the three leptons must be isolated and with a  $p_T > 10$  GeV (highest  $p_T$  above 55 GeV), a pseudorapidity  $|\eta| < 2.4$  (2.5) for the muons (electron), and an invariant mass  $m_{\mu\mu} > 5$  GeV with  $|m_{\mu\mu} - m_Z| > 15$  GeV and  $|m_{\mu\mu e} - m_Z| > 15$  GeV. We find that 20 events (just 2% of the initial HNL sample) pass the cuts for  $m_N = 90$  GeV, 17 events for  $m_N = 110$  GeV and 14 for  $m_N = 130$  GeV. The low efficiency of the cuts suggests that the CMS analysis has been optimized for larger HNL masses<sup>†</sup>.

The background, in turn, is dominated by  $WZ$  and  $ZZ$  production: we obtain that the cuts are satisfied by 285 events, which define around 50% of the total background yield [16] (*e.g.*, these 285 events do not include triboson events, leptons from heavy hadron decays nor photons and jets misidentified as leptons).

The momenta of the two muons and the electron in the HNL events can be measured, whereas the transverse momentum  $\vec{p}_T^\nu$  of the neutrino can be obtained from  $\vec{p}_T^{\text{miss}}$ . In addition, we notice that for  $m_N > m_W$  the  $W$  boson decaying into electron plus neutrino is on shell. This can be used to deduce the longitudinal momentum  $p_L^\nu$  of the neutrino (see [26], for example, for an analogous calculation in a different context): it is solution to the quadratic equation

$$(p_T^e)^2 (p_L^\nu)^2 - p_L^e (m_W^2 + 2 \vec{p}_T^e \cdot \vec{p}_T^\nu) p_L^\nu - \left( \frac{m_W^4}{4} + m_W^2 \vec{p}_T^e \cdot \vec{p}_T^\nu + (\vec{p}_T^e \cdot \vec{p}_T^\nu)^2 - (p^e)^2 (p_T^\nu)^2 \right) = 0. \quad (5)$$

With the complete momenta of the neutrino and of the electron and the muon of opposite charge (*i.e.*,  $e^\pm \mu^\mp$ ) we can now reconstruct  $m_N$ ,

$$m_N = \sqrt{(E^\mu + E^e + E^\nu)^2 - (\vec{p}^\mu + \vec{p}^e + \vec{p}^\nu)^2}. \quad (6)$$

Only one of the two solutions for  $p_L^\nu$  in Eq (5) provides the *right* reconstruction of  $m_N$ , and we find the lower one to be the best choice. In particular, when the two solutions are significantly different ( $m_2 > 1.1 m_1$ ) this is the right choice 96% of the times, whereas for similar solutions the prescription is successful 84% of the times.

In Fig. 3 we plot the distribution of the reconstructed  $m_N$  for the 20, 17 and 14 signal events that correspond to the three HNL masses together with the 285 background events (these distributions have been obtained with a normalized sample 20 times larger). Although our estimate does not include a simulation of the detector response, the peak obtained for a mixing  $|V_{\mu N}|^2 = 10^{-3}$  could be significant at the lower values of  $m_N$ .

---

<sup>†</sup>For  $m_N = 90$  GeV, in particular, we find that a reduction from 10 to 5 GeV in the minimum  $p_T$  of the least energetic lepton increases the signal by a factor of 1.42 and the background by a factor of 1.12).

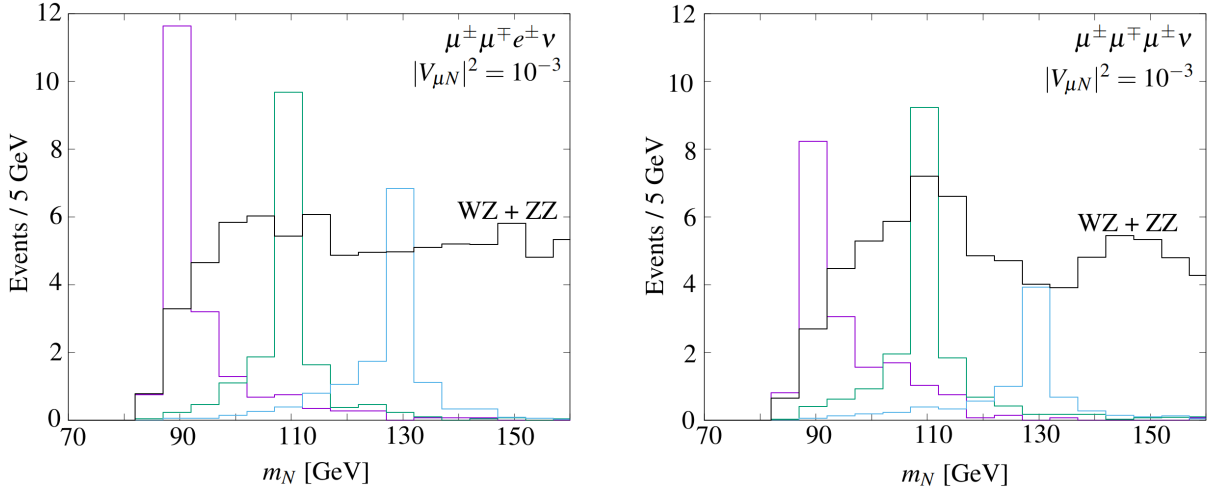


Figure 3: Mass reconstruction in  $pp \rightarrow \mu^\pm \mu^\mp e^\pm \nu$  (left) and  $pp \rightarrow \mu^\pm \mu^\mp \mu^\pm \nu$  (right) at 13 TeV,  $138 \text{ fb}^{-1}$  for  $m_N = (90, 110, 130)$  GeV with  $|V_{\mu N}|^2 = 10^{-3}$  and diboson background.

We can increase the statistics if we include the possibility that the  $W$  boson decays into a muon,

$$pp \rightarrow \mu^\pm N \rightarrow \mu^\pm \mu^\mp W^\pm \rightarrow \mu^\pm \mu^\mp \mu^\pm \nu. \quad (7)$$

In this case, the muon needed to reconstruct  $m_N$  appears together with a second muon with the same charge. We notice, however, that the production of a HNL (see Fig. 1) is favored by the collision of a valence quark and a sea antiquark in the initial protons. This tends to give a larger  $|p_L|$  to the muon in the primary vertex and, together with the cut  $p_T^{\text{miss}} > 55$  GeV, implies that  $m_N$  must be reconstructed with the muon of lower energy. The Monte Carlo simulation shows that this prescription gives the right choice 78% of the times for  $m_N = 90$  GeV or 87% for  $m_N = 130$  GeV.

Therefore we consider as well this trimuon signal. Again, we find that only 2% of the HNL events pass the cuts for  $m_N = 90$  GeV or 6% at  $m_N = 130$  GeV. The reconstruction of  $m_N$  is done with the criteria described above but changing the electron by the less energetic muon among the two with same charge. The event distribution for this observable is shown in Fig. 3-right. Combined with the dimuon plus electron events and normalizing the background by a factor of 2<sup>§</sup>, we estimate that at the current luminosity the bounds on  $|V_{\mu N}|^2$  at CMS and ATLAS could be around  $4.0 \times 10^{-4}$  for  $m_N = 90$  GeV or  $8.4 \times 10^{-4}$  for  $m_N = 130$  GeV. These limits are set at 95% confidence level using the  $CL_s$  prescription [24]. An analogous analysis for  $pp \rightarrow e^\pm N \rightarrow e^\pm e^\mp \ell^\pm \nu$  (in Fig. 4) suggests very similar bounds for the mixing with the electron flavor:  $|V_{e N}|^2 < 3.8 \times 10^{-4}$  or  $8.0 \times 10^{-4}$  for a HNL mass of 90 or 130 GeV,

<sup>§</sup>As shown in [16], triboson/top quark events, nonprompt leptons and missidentified jets/photons account approximately for 50% of the background.

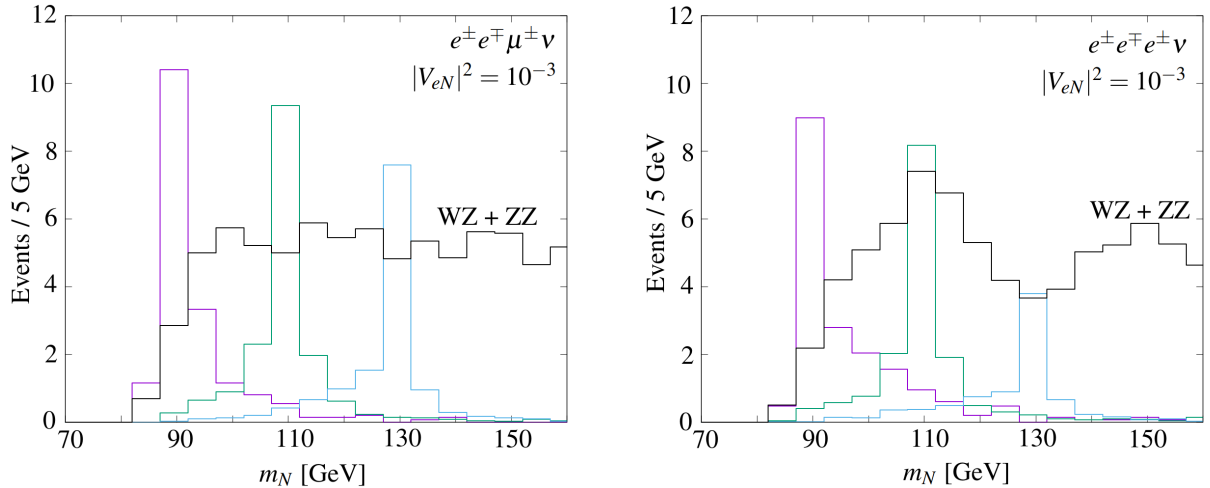


Figure 4: Mass reconstruction in  $pp \rightarrow e^\pm e^\mp \mu^\pm \nu$  (left) and  $pp \rightarrow e^\pm e^\mp e^\pm \nu$  (right) at 13 TeV,  $138 \text{ fb}^{-1}$  for  $m_N = (90, 110, 130)$  GeV with  $|V_{eN}|^2 = 10^{-3}$  and diboson background.

respectively.

### 3 Majoranas and other production channels

We can also reconstruct  $m_N$  for a heavy Majorana singlet. This case implies  $L$ -violating processes with  $p_T^{\text{miss}}$ , two muons (or electrons) with the same charge plus an electron (or muon) of opposite charge (see Fig. 1), *e.g.*,

$$pp \rightarrow W^+ \rightarrow \mu^+ N \rightarrow \mu^+ \mu^+ W^- \rightarrow \mu^+ \mu^+ e^- \bar{\nu}_e. \quad (8)$$

To reconstruct  $m_N$  we need to choose among the two same sign muons. As explained before, the muon from  $W^+ \rightarrow \mu^+ N$  tends to be the most energetic one. Here, in addition, the chirality flip in  $N$  favors that the  $\mu^+$  from  $N \rightarrow \mu^+ W^-$  is emitted backwards [27], which also reduces its energy: 89% of the times the reconstruction with the less energetic muon provides the right value for  $m_N = 110$  GeV. Again, the efficiency of the cuts seems low: 19 out of 511 HNL events pass the cuts for  $m_N = 90$  GeV or 10 out of 83 for  $m_N = 130$  GeV. We find, however, that the reconstruction of  $m_N$  *works* and, together with a total background 50% smaller than in the Dirac case, our results suggest similar limits. For example, at  $m_N = 90$  GeV we estimate

$$|V_{eN}|^2 < 4.0 \times 10^{-4}; \quad |V_{\mu N}|^2 < 4.2 \times 10^{-4}. \quad (9)$$

Finally, we would like to comment on the reconstruction of the HNL mass also in other channels. In particular, Higgs searches  $h \rightarrow WW^* \rightarrow \mu^+ \nu e^- \bar{\nu}$  (dilepton of different flavor

plus missing  $p_T$ ) [28–32] with slightly different cuts could be sensitive to the presence of the HNL:  $Z(h) \rightarrow \nu N \rightarrow \nu \mu^+ W^- \rightarrow \nu \ell^+ \bar{\nu} e^-$ .

Take  $m_N = 85$  GeV (the argument applies to any masses between  $m_W$  and around 100 GeV) and  $|V_{\mu N}|^2 = 10^{-3}$ . Before the cuts described in [33], we estimate 9,950 HNL events versus 11,320 Higgs events. We notice that the low value of  $m_N$  strongly favors that the  $s$ -channel  $Z$  boson in Fig. 2 is near the mass shell, implying that the neutrino from  $Z \rightarrow \nu N$  will carry little  $p_T$ . We can then assume that most of the missing  $p_T$  is carried by the second neutrino and, as before, use that the parent  $W$  is on shell to find  $p_L^\nu$  and reconstruct  $m_N$ . We find, however, that with the cuts optimized for Higgs searches very few  $N$  events are selected: the ones used in [33] keep only 0.7% of the 9,950 events, versus 11% of the 11,320 Higgs events. The basic reason is that the charged lepton from  $N \rightarrow \mu^+ W^-$  tends to have a  $p_T$  below the 15 GeV required to the subleading lepton. If we relax this minimum  $p_T$  to 5 GeV and impose that the electron is more energetic than the muon we would keep 1.1% of the  $N$  sample (106 events), while the fraction of  $h \rightarrow WW^*$  events passing the cuts would be reduced to 4.4% (500 Higgs events). These frequencies suggest a possible complementarity of Higgs physics and  $N$  searches in some mass region.

## 4 Discussion

In any search for a new particle it is critical to find the optimal kinematical variable that discriminates between signal and background. Here we have discussed how to reconstruct the mass of a HNL in the trilepton plus  $p_T^{\text{miss}}$  channel. This possibility may have been overlooked in several CMS analyses [15, 16], where they use a combination of observables optimized with machine learning techniques that distributes signal and background in 20 bins. Obviously, when the signal events define a mass peak its search will always be the better choice.

In another recent search for a light ( $m_N < m_W$ ) HNL [34] (see also [35]), ATLAS has reconstructed  $m_N$  using that the  $s$ -channel  $W$  in  $pp \rightarrow W^+ \rightarrow \ell^+ N$  (see Fig. 1) is near the mass shell. Since the  $W$  in  $N \rightarrow \ell^- W^+$  is exactly on shell, our analysis provides a more accurate reconstruction in the complementary regime with  $m_N > m_W$ . We have also shown that a similar reconstruction may work in the dilepton plus  $p_T^{\text{miss}}$  channel by changing the cuts currently being used in Higgs to  $WW^*$  searches.

Our estimate does not carry the degree of sophistication in these full experimental analyses, that include next to leading order corrections, the background of photons and heavy mesons misidentified as leptons, or a precise account of the detectors response. However, it seems clear that the appearance of a mass peak should simplify the search and make the de-

tails of the calculation less determinant. In summary, although it is a possibility not explored at the LHC yet, the analysis presented here suggests that the search for peaks associated to HNLs in  $pp$  collisions could probe mixings  $|V_{\ell N}|^2$  that are not excluded by PMNS unitarity bounds.

## Acknowledgments

We would like to thank Mikael Chala and José Santiago for discussions. This work has been supported by the Spanish Ministry of Science, Innovation and Universities MICIU/AEI/10.13039/501100011033/ (grants PID2022-14044NB-C21 and PID2022-139466NB-C22), by Junta de Andalucía (FQM 101) and by Unión Europea-NextGenerationEU (grant AST22\_6.5).

## References

- [1] S. Weinberg, Phys. Rev. Lett. **43** (1979), 1566-1570 doi:10.1103/PhysRevLett.43.1566
- [2] M. Fukugita and T. Yanagida, Phys. Lett. B **174** (1986), 45-47 doi:10.1016/0370-2693(86)91126-3
- [3] S. Dodelson and L. M. Widrow, Phys. Rev. Lett. **72** (1994), 17-20 doi:10.1103/PhysRevLett.72.17 [arXiv:hep-ph/9303287 [hep-ph]].
- [4] A. Atre, T. Han, S. Pascoli and B. Zhang, JHEP **05** (2009), 030 doi:10.1088/1126-6708/2009/05/030 [arXiv:0901.3589 [hep-ph]].
- [5] V. Tello, M. Nemevsek, F. Nesti, G. Senjanovic and F. Vissani, Phys. Rev. Lett. **106** (2011), 151801 doi:10.1103/PhysRevLett.106.151801 [arXiv:1011.3522 [hep-ph]].
- [6] A. Das and N. Okada, Phys. Rev. D **88** (2013), 113001 doi:10.1103/PhysRevD.88.113001 [arXiv:1207.3734 [hep-ph]].
- [7] A. Boyarsky, M. Drewes, T. Lasserre, S. Mertens and O. Ruchayskiy, Prog. Part. Nucl. Phys. **104** (2019), 1-45 doi:10.1016/j.ppnp.2018.07.004 [arXiv:1807.07938 [hep-ph]].
- [8] M. Drewes, J. Klarić and J. López-Pavón, Eur. Phys. J. C **82** (2022) no.12, 1176 doi:10.1140/epjc/s10052-022-11100-7 [arXiv:2207.02742 [hep-ph]].
- [9] A. J. Cuesta, M. E. Gómez, J. I. Illana and M. Masip, JCAP **04** (2022) no.04, 009 doi:10.1088/1475-7516/2022/04/009 [arXiv:2109.07336 [hep-ph]].

- [10] P. de la Torre, M. Gutiérrez and M. Masip, JCAP **11** (2023), 068 doi:10.1088/1475-7516/2023/11/068 [arXiv:2309.00374 [hep-ph]].
- [11] R. N. Mohapatra and J. W. F. Valle, Phys. Rev. D **34** (1986), 1642 doi:10.1103/PhysRevD.34.1642
- [12] E. Fernandez-Martinez, J. Hernandez-Garcia and J. Lopez-Pavon, JHEP **08** (2016), 033 doi:10.1007/JHEP08(2016)033 [arXiv:1605.08774 [hep-ph]].
- [13] G. Hernández-Tomé, G. López Castro and P. Roig, Eur. Phys. J. C **79** (2019) no.1, 84 [erratum: Eur. Phys. J. C **80** (2020) no.5, 438] doi:10.1140/epjc/s10052-019-6563-4 [arXiv:1807.06050 [hep-ph]].
- [14] G. Hernández-Tomé, J. I. Illana, M. Masip, G. López Castro and P. Roig, Phys. Rev. D **101** (2020) no.7, 075020 doi:10.1103/PhysRevD.101.075020 [arXiv:1912.13327 [hep-ph]].
- [15] A. M. Sirunyan *et al.* [CMS], Phys. Rev. Lett. **120** (2018) no.22, 221801 doi:10.1103/PhysRevLett.120.221801 [arXiv:1802.02965 [hep-ex]].
- [16] A. Hayrapetyan *et al.* [CMS], [arXiv:2403.00100 [hep-ex]].
- [17] P. Achard *et al.* [L3], Phys. Lett. B **517** (2001), 67-74 doi:10.1016/S0370-2693(01)00993-5 [arXiv:hep-ex/0107014 [hep-ex]].
- [18] C. Degrande, C. Duhr, B. Fuks, D. Grellscheid, O. Mattelaer and T. Reiter, Comput. Phys. Commun. **183** (2012), 1201-1214 doi:10.1016/j.cpc.2012.01.022 [arXiv:1108.2040 [hep-ph]].
- [19] A. Alloul, N. D. Christensen, C. Degrande, C. Duhr and B. Fuks, Comput. Phys. Commun. **185** (2014), 2250-2300 doi:10.1016/j.cpc.2014.04.012 [arXiv:1310.1921 [hep-ph]].
- [20] J. Alwall, R. Frederix, S. Frixione, V. Hirschi, F. Maltoni, O. Mattelaer, H. S. Shao, T. Stelzer, P. Torrielli and M. Zaro, JHEP **07** (2014), 079 doi:10.1007/JHEP07(2014)079 [arXiv:1405.0301 [hep-ph]].
- [21] C. Bierlich, S. Chakraborty, N. Desai, L. Gellersen, I. Helenius, P. Ilten, L. Lönnblad, S. Mrenna, S. Prestel and C. T. Preuss, *et al.* SciPost Phys. Codeb. **2022** (2022), 8 doi:10.21468/SciPostPhysCodeb.8 [arXiv:2203.11601 [hep-ph]].

[22] M. Cacciari, G. P. Salam and G. Soyez, Eur. Phys. J. C **72** (2012), 1896 doi:10.1140/epjc/s10052-012-1896-2 [arXiv:1111.6097 [hep-ph]].

[23] R. Brun and F. Rademakers, Nucl. Instrum. Meth. A **389** (1997), 81-86 doi:10.1016/S0168-9002(97)00048-X

[24] A. L. Read, J. Phys. G **28** (2002), 2693-2704 doi:10.1088/0954-3899/28/10/313

[25] A. Buckley, P. Ilten, D. Konstantinov, L. Lönnblad, J. Monk, W. Pokorski, T. Przedzinski and A. Verbytskyi, Comput. Phys. Commun. **260** (2021), 107310 doi:10.1016/j.cpc.2020.107310 [arXiv:1912.08005 [hep-ph]].

[26] P. Sanyal and D. Wang, JHEP **09** (2023), 076 doi:10.1007/JHEP09(2023)076 [arXiv:2305.00659 [hep-ph]].

[27] J. Shelton, Phys. Rev. D **79** (2009), 014032 doi:10.1103/PhysRevD.79.014032 [arXiv:0811.0569 [hep-ph]].

[28] M. Aaboud *et al.* [ATLAS], Phys. Lett. B **789** (2019), 508-529 doi:10.1016/j.physletb.2018.11.064 [arXiv:1808.09054 [hep-ex]].

[29] G. Aad *et al.* [ATLAS], Phys. Lett. B **798** (2019), 134949 doi:10.1016/j.physletb.2019.134949 [arXiv:1903.10052 [hep-ex]].

[30] A. M. Sirunyan *et al.* [CMS], JHEP **03** (2021), 003 doi:10.1007/JHEP03(2021)003 [arXiv:2007.01984 [hep-ex]].

[31] G. Aad *et al.* [ATLAS], Eur. Phys. J. C **82** (2022) no.7, 622 doi:10.1140/epjc/s10052-022-10366-1 [arXiv:2109.13808 [hep-ex]].

[32] G. Aad *et al.* [ATLAS], Eur. Phys. J. C **83** (2023) no.9, 774 doi:10.1140/epjc/s10052-023-11873-5 [arXiv:2301.06822 [hep-ex]].

[33] A. Tumasyan *et al.* [CMS], Eur. Phys. J. C **83** (2023) no.7, 667 doi:10.1140/epjc/s10052-023-11632-6 [arXiv:2206.09466 [hep-ex]].

[34] G. Aad *et al.* [ATLAS], Phys. Rev. Lett. **131** (2023) no.6, 061803 doi:10.1103/PhysRevLett.131.061803 [arXiv:2204.11988 [hep-ex]].

[35] C. O. Dib, C. S. Kim and K. Wang, Phys. Rev. D **95** (2017) no.11, 115020 doi:10.1103/PhysRevD.95.115020 [arXiv:1703.01934 [hep-ph]].